IEEE Access
Multidisciplinary | Rapid Review | Open Access Journal

Received June 16, 2018, accepted August 6, 2018, date of publication August 27, 2018, date of current version September 21, 2018.

Digital Object Identifier 10.1109/ACCESS.2018.2867220

Ionic Conductive Polyurethane-Graphene Nanocomposite for Performance Enhancement of Optical Fiber Bragg Grating Temperature Sensor

FAREEZA JASMI[1], NUR HIDAYAH AZEMAN[1], AHMAD ASHRIF A. BAKAR[1], (Senior Member, IEEE), MOHD SAIFUL DZULKEFLY ZAN[1], (Member, IEEE), KHAIRIAH HAJI BADRI[2], AND MOHD SUKOR SU'AIT[3]

[1]Center of Advanced Electronic and Communication Engineering, Faculty of Engineering and Built Environment, Universiti Kebangsaan Malaysia, 43600 Bangi, Malaysia
[2]Faculty of Science and Technology, School of Chemical Sciences and Food Technology, Universiti Kebangsaan Malaysia, 43600 Bangi, Malaysia
[3]Solar Energy Research Institute, Universiti Kebangsaan Malaysia, 43600 Bangi, Malaysia

Corresponding authors: Nur Hidayah Azeman (nhidayah.az@ukm.edu.my), Mohd Saiful Dzulkefly Zan (saifuldzul@ukm.edu.my), and Mohd Sukor Su'ait (mohdsukor@ukm.edu.my)

This work was supported in part by the Undergraduates Research Fund through the Electrical and Electronic Engineering Program, in part by the Faculty of Engineering and Built Environment, UKM, under Grant DIP-2017-003, and in part by the UKM Top-Down Research under Grant TD-2015-008.

ABSTRACT Polyurethane-graphene (PU-graphene) nanocomposite was utilized as the sensing material for a fiber Bragg grating (FBG) temperature sensor. The nanocomposite was characterized using a Fourier transform infrared spectroscopy (FTIR), thermogravimetric analysis (TGA), scanning electron microscopy (SEM), and electrochemical impedance spectroscopy (EIS) to study the morphology and physical properties of the materials for FBG temperature sensing application. The physical, chemical, and conductivity of PU-graphene improve after graphene was introduced in pristine PU. The FTIR shows that the strong intermolecular interaction between –O–C = O (ester) and hydrogen in graphene in the PU-graphene was indicated by the shift to lower wavenumber of ether (C–O–C) peak at ∼1220 cm^{-1} to ∼1218 cm^{-1}. TGA shows the thermal stability of PU increases to 217 °C due to the strong intermolecular interaction with the presence of graphene flakes. EIS shows a good electrical conductivity of 1.39 × 10^{-9} Scm^{-1} in the PU-graphene due to the electron transfer provided by the graphene. The SEM shows a rough and uneven texture on the surface of FBG coated by PU-graphene nanocomposite which shows that the graphene flakes are completely coated by polyurethane polymer. The PU-graphene was then dip-coated on the optical fiber-based Bragg grating, and the sensor performance for a temperature sensor was evaluated, where a good linearity with the sensitivity of 6 pm/°C was achieved.

INDEX TERMS Fiber Bragg grating, graphene, polyurethane, temperature sensor.

I. INTRODUCTION

Fiber Bragg Grating (FBG) as an optical sensor has been widely applied in various fields for measurement of numerous parameters, such as temperature, pressure, strain and motion. It has been used extensively for temperature measurement in various industrial control system processes [1], [2]. FBG is known as an optical filtering device, reflecting optical signals at a certain wavelength within the core of an optical fiber [3], [4]. Simple fabrication, light weight, immunity to electromagnetic interference and long-range monitoring system are the highlights of the FBGs to be utilized as a promising sensor [5]. However, the low thermal expansion coefficient of silica with the variation of temperature is a major drawback of bare FBG application in temperature sensing which makes the sensor less sensitive [5]. A normalized responsivity of 6.67 x 10^{-6} $°C^{-1}$ was reported for a bare FBG with 1.3 μm wavelength over the range of 5°C to 85 °C. Previous studies reported that there are two factors affecting the dependence of the Bragg wavelength towards temperature: (i) the dependence of the glass refraction index towards temperature and (ii) the glass thermal expansion [6]. Basically, an FBG is not very sensitive towards the external changes of the refractive index, hence the thermal sensitivity of the FBG sensor can be improved by the application of

different types of coating materials such as polymer and metal whose thermal expansion coefficient is greater than silica [2], [5], [7]. The sensitivity of the FBG wavelength to temperature can be controlled by the thermal characteristics of the coating materials [1].

Li *et al*. [8] have reported that the temperature sensitivity of FBG sensor could be enhanced by using nickel metal as coating material. Wu *et al.* in [9] claimed that by introducing capillary steel tubes, metalized and organic polymer packages can enhance the sensitivity of the FBG sensor for the low temperature measurements down to 0.0213 nm/°C, 0.0283 nm/°C and 0.1376 nm/°C, respectively. Recently, Park *et al*. [5] used FBG with coated poly-dimethylsiloxane (PDMS) for sensitivity enhancement due to the higher thermal expansion coefficient possessed by PDMS in comparison to metal. Better sensitivity was reported for a higher cross-section areas (A_p) of the PDMS jackets with 0.026 nm/°C (for $A_p = 25$ mm^2), 0.033 nm/°C (for $A_p = 100$ mm^2), 0.042 nm/°C (for $A_p = 400$ mm^2).

Ionic conductive solid polymer electrolytes possess both mechanical properties of polymers and electrical properties of conductors which are excellent for the development of electronic and optical devices. Features such as, high electrical conductivity, ease of synthesis, good thermal and environmental stability make them superior compared to other conductive materials for instance carbon nanotubes and their derivatives [10].

Polyurethane (PU) is a type of a conductive polymer consists of polyols and isocyanates in its polymeric chain structure. The soft and hard segments in the PU polymeric chain is due to the presence of polyols and isocyanates respectively [11]. The PU soft segment act as a polymer solvent to solvate the cations favoring the transportation of the ions hence contribute to the conductivity of the PU. Meanwhile, the PU hard segment act as supporting fillers, whereby it is interconnected throughout the soft phase segment, henceforth contribute to the mechanical strength of the PU [12] and to preserve the stability of the sensor [13].

Superior electrical conductivity is the most imperative element of graphene. Graphene is a sp^2-hybridized single layer, which also well-known for its high thermal conductivity as well as excellent mechanical properties [14]. Recently, the incorporation of graphene into PU greatly improved the physical, chemical and conductivity of the polymer composite [15], because of the covalent bond formation between the hydroxyl groups at the surfaces of graphene with the isocyanate groups of PU chain [14]. Pokharel *et al*. [16] reported many hydroxyl groups on the surface of graphite derivatives offers abundant active sites for the covalent grafting of PU onto the surface of graphite derivatives, thus PU interact more effectively with the graphite derivatives for effective load transfer.

In this work, a Type 1 uniform grating FBG was used. It has a wavelength, length, period and reflectivity of 1550.233 nm, 10 mm, 530.90 nm and 99.38 %, respectively. The detailed specifications of the FBG used in this study were given in Appendix A. The small segment of FBG (2.5 cm – 3.0 cm) was dip-coated with bio-based polyurethane (PU) synthesized from palm kernel oil-based monoester-OH (PKO-p) doped with graphene for the development of temperature sensor. The coating material was synthesized and characterized by using attenuated total reflection Fourier transform infrared (ATR-FTIR) spectroscopy, temperature dependence electrochemical impedance spectroscopy (EIS), thermogravimetric analysis (TGA) and scanning electron microscopy (SEM) to study the morphology and physical properties of the materials for FBG sensor application. The performance of the PU-graphene nanocomposite as a coating material for temperature sensor was evaluated at different temperature using FBG sensor based on the observation of changes in refractive index (RI) of the transducer. The sensitivity and stability of the non-coated FBG, FBG coated with PU and FBG coated with PU-graphene were studied.

II. MATERIALS

2,4′-Methylene diphenyl diisocyanate (MDI) was commercially obtained from Cosmopolyurethane Sdn. Bhd. (Malaysia). Palm kernel oil-based monoester-OH (PKO-p) were synthesized by polyesterification reaction in UKM laboratory using established method by Wong and Badri [17]. Graphene flakes was supplied by KGC Sdn, Bhd. (Malaysia). Acetone and ethanol 99.9 % were supplied by SYSTERM ChemAR (Poland).

III. SYNTHESIS AND PREPARATION OF BIO-BASED POLYURETHANE

Polyurethane polymer was synthesized by pre-mixed palm kernel oil-based monoester-OH (PKO-p) in 5 mL of acetone and stirred for 1 h. Afterward, the graphene powder was dispersed in PKO-p solution using magnetic stirrer for the first 1 h and the dispersion was prolonged using Vortex mixer for another 20 minutes to improve homogeneous distribution of the graphene in PKO-p solution. The PU-graphene nanocomposite was prepared via *in-situ* addition polymerization of isocyanate ends segment to hydroxyl groups of PKO-p. The 2,4′-methylene diphenyl diisocyanate (MDI) was dissolved in 5 mL acetone solution for 1 h prior to PU synthesis. The solution was later added into PKO-p–graphene mixture under continuous stirring (5000 – 6000 rpm) for 1 h. The reaction was conducted at ambient temperature under nitrogen gas atmosphere in a glass vessel. The mixture was stirred for an hour before casted onto Teflon mould in glovebox and allowed to evaporate at room temperature. The produced films were kept in the desiccator for further characterization.

IV. CHARACTERISATION OF THE MATERIAL

A. ATTENUATED TOTAL REFLECTION-FOURIER TRANSFORM INFRARED SPECTROSCOPY (ATR-FTIR) ANALYSIS

ATR-FTIR analysis was recorded by computer interfaced with Perkin Elmer 2000. The films were placed onto ATR crystal and analyzed in the frequency range of 4000 cm^{-1} to

650 cm^{-1} at a scanning resolution of 2 cm^{-1}. The purpose of this analysis was to observe the functional groups and chemical interaction in the system.

B. THERMAL ANALYSIS

Thermogravimetric analysis was carried out using a Mettler–Toledo TGA/SDTA 851 instrument under nitrogen gas atmosphere from room temperature to 600°C at a heating rate of 10 °C/min. A sample of mass ∼5 mg was used to determine the weight loss of the polymers.

C. IMPEDANCES ANALYSIS

The dielectric studies of the PU membranes were carried out by alternating current (AC) electrochemical impedance spectroscopy (EIS) Princeton Model VERSASTAT4 using a frequency resonance analyzer (FRA) with applied frequency from 1 MHz to 0.01 Hz at 100 mV amplitude. The 16 mm in diameter disc-shaped sample was sandwiched between two stainless steel block electrodes. All the electrical parameters were extracted from the Nyquist plot given by EIS measurement.

D. RESISTIVITY AND ELECTRICAL CONDUCTIVITY

The resistivity was obtained by the equation, $\rho = [(A.R_b)/l]$ and the electrical conductivity $\sigma = 1/\rho$. Bulk resistance (R_b) was determined from the equivalent circuit analysis by using the Z_{view} analyzer software, contact area of the thin film ($A = 1.77\ cm^2$), and average thickness of 0.01 cm (measured by Mitoyo digital caliper).

E. ELECTRICAL MODULUS

Electrical modulus (M^*) is an effective tool to predict the relaxation behavior of conducting polymeric materials. The essential quantities in impedances spectroscopy given by the modulus function in equation (1) and (2):

$$M_i(\omega) = \varepsilon_r/(\varepsilon_{r^2} + \varepsilon_{i^2}) \quad (1)$$

$$M_r(\omega) = \varepsilon_r/(\varepsilon_{r^2} + \varepsilon_{i^2}) \quad (2)$$

Where ε_i is the dielectric loss, ε_r is dielectric constants and ω is $2\pi f$, f is the frequency in Hz.

V. FBG FABRICATION

FBG sensor was cleaved with a cleaver to ensure the end tip of the FBG is perpendicular (90°) with the length of the FBG. The FBG was cleaned with ethanol to remove the dust on the surface of the FBG before coated with PU-graphene nanocomposite. The FBG was dip-coated with PU-graphene nanocomposite by using a dip coating technique from the mould in the glovebox with the aid of the programmable dip coater machine (PTL-MMB01, MTI Corporation, United States). The speed of the dip coater machine was fixed at 200 mm/min for all the samples analyzed. Flow chart of the sensing layer coating process was provided in Appendix B.

The performance of the FBG sensor was carried out to study the sensitivity of the FBG sensor. Figure 1 shows the setup for the FBG fabrication. Based on the figure, the light was released from a broadband source into the optical fiber and the spectrum of the reflected light was analyzed. In this system, the optical circulator was used to transmit the emitted light into the transmission fiber and redirect the reflected light back to the optical spectrum analyzer. The wavelength shift was observed as the temperature was varied.

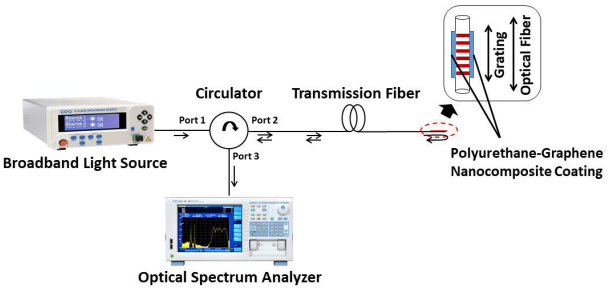

FIGURE 1. Experimental setup for FBG temperature sensor.

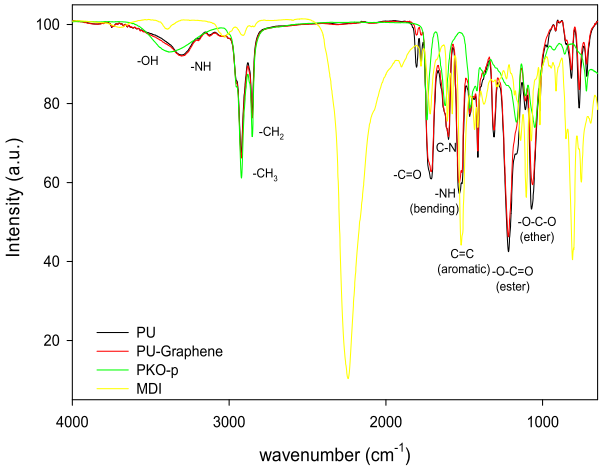

FIGURE 2. FTIR spectra for pristine PU and PU-graphene nanocomposite.

VI. RESULTS AND DISCUSSION

A. ATR-FTIR

ATR-FTIR analysis in Figure 2 indicates the disappearance of isocyanate (NCO) peak of MDI around ∼2230 cm^{-1} shows that diisocyanate is reacted completely with PKO-p polyols. This signifies that free diisocyanate is removed completely during nucleophilic substitution reactions by amine functional groups in PKO-p as nucleophile [17]. The disappearance of –OH stretching mode which belongs to hydroxyl groups of PKO-p at 3387 cm^{-1} and the presence of single band stretching mode of (–NH) peaks appear at 3300 cm^{-1} further prove the presence of secondary amides (–NHCO–) of PU in the polymeric structure [17]. Furthermore, the existences of stretching mode of carbonyl urethane group (–C = O) (∼1709 cm^{-1}) and carbamate group (C–N and –O–C = O (ester)) (∼1600 cm^{-1} and ∼1220 cm^{-1}) confirm a success formation of PU [18].

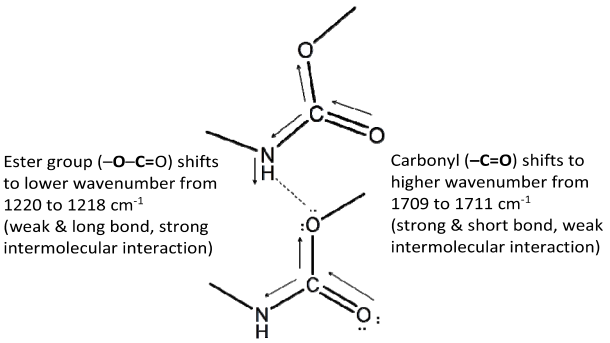

FIGURE 3. Proposed schematic of physical crosslink between urethane linkages.

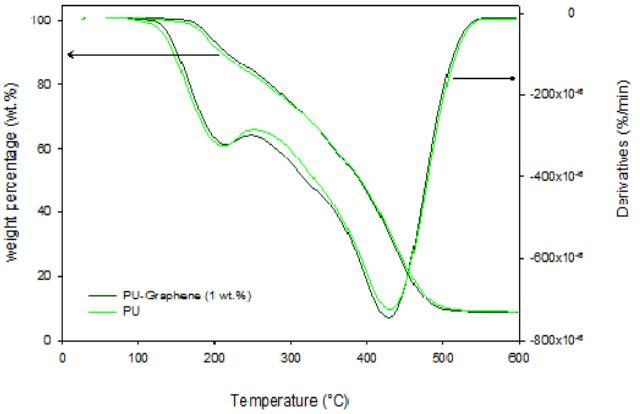

FIGURE 4. TGA analysis for pristine PU and PU-graphene nanocomposite.

TABLE 1. Thermal properties of pristine PU and PU-Graphene nanocomposite.

Sample	Thermal decomposition (Td_1)	Weight loss (wt.%)	Thermal decomposition (Td_2)	Residue (wt.%)
Pristine PU	204	41.38	432	8
PU-Graphene	217	46.08	427	8

The functional group of carbonyls (–C = O) for tertiary amides of monoester polyols PKO-p is observed at 1738 cm^{-1} is independent of its physical state as it is not possible to form hydrogen bonding with another tertiary amide group [19]. Whereas, with the presence of graphene flakes, the stretching mode of carbonyl urethane group (–C = O) and bending mode of –NH (amide) shifted from ∼1709 cm^{-1} and 1530 cm^{-1} to higher wavenumber, ∼1711 cm^{-1} and 1532 cm^{-1}, respectively.

After the addition of graphene, the ether (–O–C–O) peak at ∼1220 cm^{-1} is shifted to ∼1218 cm^{-1}. The lower frequencies absorption indicates that the stronger intermolecular interaction (physical crosslink) between hydrogen in graphene and –O–C = O (ester)) led to shorter bond in –C = O stretching mode vibration. Thus, produce more brittle coating on FBG fiber due to the increase of crystallinity. The proposed mechanism in Figure 3 indicates how intermolecular interaction; hydrogen bond is greatly affected by the presence of graphene flakes. Notably, with the presence of graphene, the physical crosslink between urethane is identified to weaken physical-chemical interaction observed in PU as indicated by unaffected single band stretching mode of (−NH) at 3300 cm^{-1}.

B. THERMAL ANALYSIS

Thermal analyses were carried out to determine the thermal stability and phase transition of the materials. The degree of crystallinity is found to be increased with the presence of graphene and T_m is insignificantly increased from 102 °C to 103 °C. Whereas, two glass transition temperature was identified; T_g PU = 40 °C, 77 °C and T_g PU-graphene 47 °C, 65 °C. The thermal decomposition stage (T_d) of pristine PU and PU-graphene nanocomposite occur at two stages as can be seen in Figure 4 and summarized in Table 1. The first decomposition (T_{d1}) stage of pristine PU was started at 120 °C and reached its maximum (T_{max}) at 204 °C due to degradation of the hard-segmented block co-polymer of the urethane linkages that resulted to the three decomposition mechanisms for urethane bonds: (i) dissociation to isocyanate and alcohol, (ii) formation of primary amine, carbon dioxide and (iii) formation of secondary amine and carbon dioxide [20]–[22]. With the addition of graphene flakes, thermal stability of PU increased to 217 °C with higher weight loss. A relatively strong intermolecular force in semi-crystallinity PU-graphene nanocomposite requires higher temperature to disruption even above the glass transition temperature. The increase in thermal stability and glass transition temperature may also due to the thermally conductive properties of graphene as its unique two-dimensional structure, further offers a lower thermal resistance between the surfaces.

Fundamentally, the percolation theory can be applied to analyses the thermal conductivity in nanocomposites; in amorphous polymer, phonons (lattice vibrations) are known as the major mode of thermal conduction. The phonon scattering at the filler-matrix and interface can be reduced by the formation of physical/chemical bond between the filler and matrix, thus enhance the thermal conductivity of nanocomposites [23]. Whereas, the second degradation (T_{d2}) stage begins at T_{d2} = 251 °C with T_{max} = 432 °C where later reduced after the addition of graphene. The T_{d2} degradation is contributed by the thermal decomposition of soft segments of PU (ester linkages), which was seldom affected by the chemical composition and the three-dimensional arrangement of polyurethane structure [20], [24]. The degradation region corresponds to the liberation of free isocyanate at the range of 240-370 °C is not observed probably due to overlapping peak [11], [25]. Although T_{d1}, and T_{d2} shifted significantly but the residue after 600 °C decomposition is equivalent to both samples [24].

C. RESISTIVITY AND ELECTRICAL CONDUCTIVITY

Electrochemical impedance spectroscopy (EIS) was carried out to study the influence of the governing physical and

TABLE 2. Conductivity of pristine PU and PU-Graphene nanocomposite.

Sample	Bulk Resistance (Ω)	Resistivity (Ωcm) (wt.%)	Conductivity (Scm^{-1})	Dielectric Constant (10 Hz, 25°C)
Pristine PU	$1.50x10^{8}$	$1.06x10^{-12}$	$9.43x10^{-11}$	8
PU-Graphene	$5.09x10^{9}$	$7.19x10^{-10}$	$1.39x10^{-9}$	59

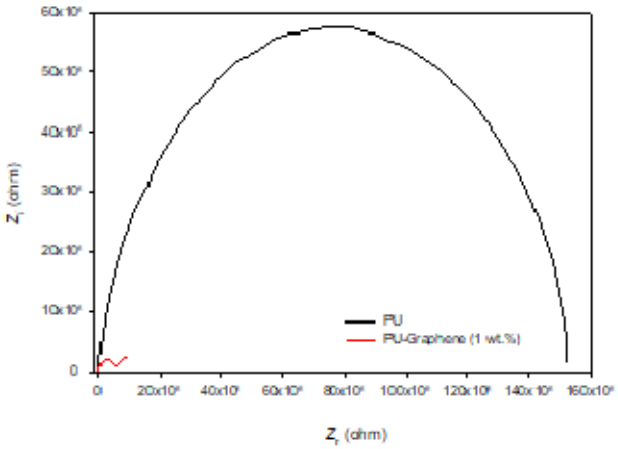

FIGURE 5. Electrochemical impedance spectrum for pristine PU and PU-graphene at ambient temperature.

chemical phenomena that may be isolated and distinguished at a given applied frequency. Table 2 shows electrical properties of pristine PU and PU-graphene nanocomposites, whereas Figure 5 indicates the impedance spectra for both samples. According to Nyquist plot, the pristine PU sample has higher resistance than PU-graphene sample [26], which indicates the insulating properties of pristine PU. With addition of graphene, the conductivity was increased two magnitudes, from 9.43×10^{-11} Scm^{-1} to 1.39×10^{-9} Scm^{-1} at ambient temperature. The conductivity was clearly affected by the electron transfer provide highly electrically conductive, graphene, where it forms a network that led to an increase in the electrical conductivity of composites [27]. This proves that the addition of graphene as a filler in PU managed to increase the conductivity of composite coatings on optical FBG-based compared to fiber without graphene-coating.

D. ELECTRICAL MODULUS

Dielectric relaxation studies of polymeric materials are related to the relaxation of dipoles in polymeric host. Dielectric constant is a measure of the amount of charge stored. The observed variation in ε_r with frequency could be attributed to the formation of a space charge region at the electrode and electrolyte interface at the low frequency region.

This behavior is known as the non-Debye type of behavior, where diffusion of ions occurs in the space charge regions [28]. The increase in the dielectric constant and

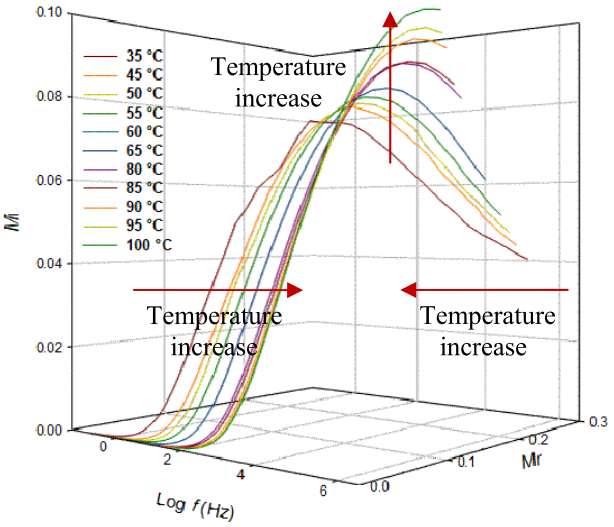

FIGURE 6. Electrical modulus behavior of PU-graphene nanocomposites at applied frequency between 30 to 100 °C.

dielectric loss with temperature can be attributed to the increase in charge carrier density at the space charge accumulation region, which causes equivalent capacitance to be enhanced [29]. The low frequency dispersion region corresponds to the contribution of charge accumulation at the electrode–electrolyte interface.

At high frequencies, the periodic reversal of the electric fields occurs so fast that there is no time for ion to build up at the interface. Hence, the polarization due to the charge accumulation decreases, which caused the decrease in the value of εr [30]. Figure 6 shows electrical modulus behavior of PU-graphene nanocomposites at applied frequency between 30 to 100 °C. The complete analysis of electrical properties for pristine PU and PU-graphene nanocomposite is provided in supplementary material (Figure S3-S6).

E. CONDUCTIVITY DEPENDENCE ON TEMPERATURE

Figure 7 shows the conductivity, σ dependence on temperature, T curve for the PU-graphene nanocomposite sample. According to Figure 7, the conductivity of PU-graphene increased when the temperature is raised [30]. The relationship between conductivity and temperature for PU-graphene nanocomposite was found to be linear with the regression line of 0.9916 which obeyed Vogel-Tamman Fulcher (VTF) equation, which given by the equation (3) below:

$$\sigma = AT^{-(\frac{1}{2})} exp^{(\frac{-B}{k}(T-T_o))} \tag{3}$$

where, A = $m1$ = pre-exponential factor (σ_0), B = $m2$ = pseudo activation energy (E_a), $m3 = T_o$ (temperature).

Vogel-Tamman Fulcher rule is applied as a part of the analysis on the temperature reliance of the consistency of the fluid or unwinding time, dispersion coefficient and electrical conductivity in a wide assortment of liquids including metallic glass framing materials. Its condition is frequently used to portray the behavior observed particularly in the

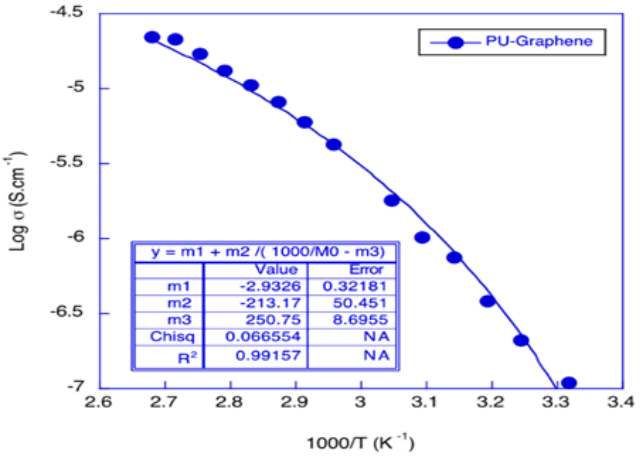

FIGURE 7. Conductivity, σ dependence on temperature, T plots for the PU-graphene nanocomposite.

fragile system. Pseudo-activation energy (E_a) is found at $E_a = 42.2$ eV, which regarded as the minimum amount of energy needed before the electron can move from one position to another. Whereas, the pre-exponential factor (σ_0) $= 1.2 \times 10^{-3}$ Scm^{-1} is related to the number of charges at the maximum point. The electrical conductivity symbolizes electron mobility of the overall polymer where it might be controlled by the free volume which leads to an expansion in electron mobility and segmental that help to transport particles or electrons.

F. MORPHOLOGICAL STUDY

PU-graphene was integrated with optical fiber-based Grating and the scanning electron microscopy (SEM) was carried out to study the surface morphology of the samples. Figure 8 shows the SEM micrograph of FBG coated with (a) pristine PU and (b) PU-graphene nanocomposite. A smooth surface was observed for FBG coated with PU without graphene as can be seen in Figure 8(a). However, an inhomogeneous, rough and uneven texture was observed on the surface of FBG coated with PU-graphene nanocomposite in Figure 8(b), which clearly shows visible flakes of graphene on FBG surface coating. The dispersion of graphene flakes can be improved by using ultrasonic dispenser, sputter coating, etching or immersion technique to obtain more even texture on the surface of the FBG. Figure 9 shows the SEM micrograph for FBG coated with PU-graphene nanocomposite at 5000X magnification. It shows that graphene flakes are completely coated by polyurethane polymer, thus improves the thermal conduction of the FBG. The bright and dark tones on the surface topography represent the crystalline and amorphous phase structures respectively.

G. FIBRE BRAGG GRATING FOR TEMPERATURE SENSOR

In this work, various range of temperatures were carried out to observe the effect towards FBG wavelength using FBG coated with pristine PU and PU-graphene nanocomposite.

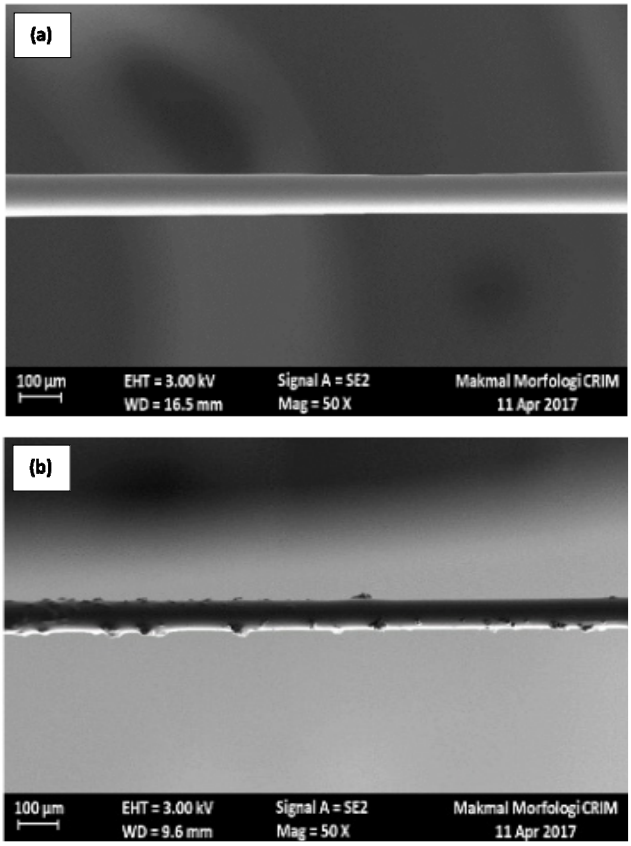

FIGURE 8. SEM images of FBG coated with (a) pristine PU and (b) PU-graphene nanocomposite.

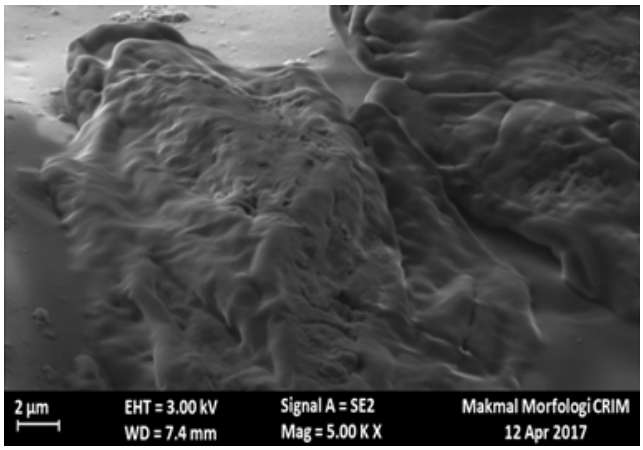

FIGURE 9. Surface morphology of FBG coated with PU-graphene.

The grating period and index of refraction of the optical fiber is highly dependent on the temperature variation, hence produce different value of Bragg wavelength [1] due to the thermal expansion of the fiber and strain induced by thermal expansion of the pristine PU and PU-graphene nanocomposite coatings [7].

Figure 10(a) and (b) shows the Bragg grating power based optical fiber using pristine PU and PU-graphene

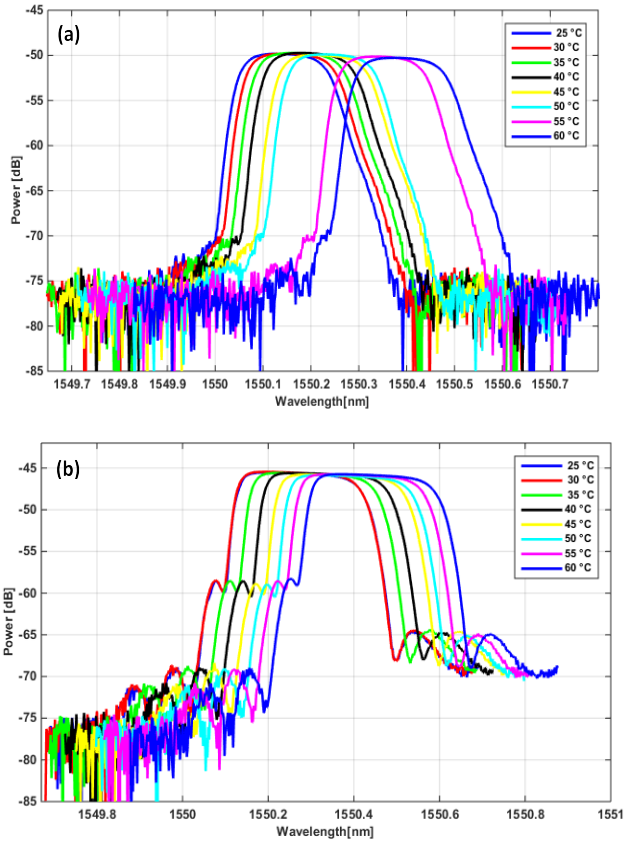

FIGURE 10. The wavelength shift of FBG coated with (a) pristine PU and (b) PU-graphene nanocomposite at various temperature

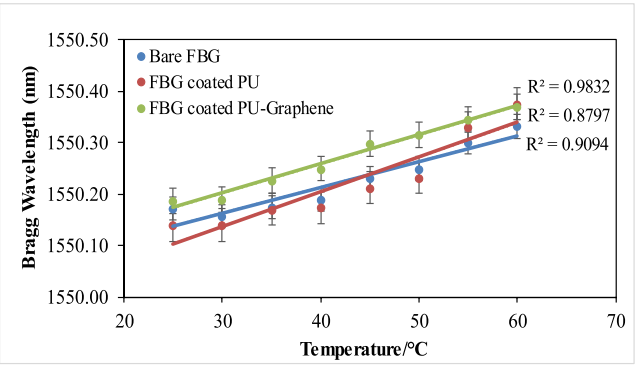

FIGURE 11. Calibration plot for bare FBG, FBG coated with pristine PU and FBG coated with PU-graphene nanocomposite.

nanocomposite with the power value of −50 dB and −45 dB respectively. The power value was increased from −50 dB to −45 dB when pristine PU was substituted with PU-graphene nanocomposite as the coating material. The graph trend of the wavelength changes for FBG coated with pristine PU as seen in Figure 10(a) is not uniform in contrast to the wavelength change in FBG coated with PU-graphene nanocomposite. The gradual raised in temperature causes the constant change in wavelength for the FBG coated with PU-graphene nanocomposite. Furthermore, the adjacent wavelength peaks were more prominent as the graphene were introduced in the later FBG coated optical fiber as seen in Figure 10(b). Interestingly, these adjacent peaks can be used as alternative for calculating the wavelength shift of the peak for FBG coated with PU-graphene, which is not observed in the FBG coated with pristine PU graph.

H. SENSOR SENSITIVITY

Figure 11 shows the difference in wavelength dependence on temperature for non-coated FBG, FBG coated with pristine PU and FBG coated with PU-graphene nanocomposite. The FBG sensitivity was calculated to be 6 pm/°C for FBG coated with PU-graphene nanocomposite. According to Figure 11, a good linearity was depicted for FBG coated with PU-graphene nanocomposite ($R^2 = 0.9832$) within the temperature range of 25 °C to 60 °C, hence shows better sensitivity and good stability for this material compared to non-coated FBG ($R^2 = 0.9094$) and FBG coated with pristine PU ($R^2 = 0.8797$).

The surface of the FBG is made of silica, which has low thermal expansion coefficient and leads to low sensitivity to temperature [5]. By coating the bare FBG with PU material which has higher thermal expansion coefficient than silica improves the sensor sensitivity. Furthermore, by the addition of the graphene flakes into pristine PU, the stability of this material increases due to the strong intermolecular force in semi-crystallinity PU-graphene nanocomposite as confirmed by the TGA analysis in Figure 4.

The stability of the material affects the sensitivity of the temperature sensor. Hence, the sensitivity of the material increases at higher temperature in comparison to the pristine PU. Consequently, the FBG coated with PU-graphene nanocomposite has a good potential for the temperature sensor application with the sensitivity of 6 pm/°C.

VII. CONCLUSION

The material characterization results confirm that the polyurethane-graphene was successfully synthesized. The addition of graphene in PU greatly improves the properties of PU-graphene nanocomposite. A better thermal stability was observed for PU-graphene with 217 °C. The electron conductivity of the coating material increases from 9.43×10^{-11} Scm^{-1} to 1.39×10^{-9} Scm^{-1}. The increase power of 5 dB was observed when PU-graphene nanocomposite was used as the coating material in FBG sensor. A good linearity was obtained for FBG coated with PU-graphene nanocomposite with the sensitivity of 6 pm/°C, hence suitable to be applied as a temperature sensor for various applications.

ACKNOWLEDGMENT

The authors would like to extend their gratitude towards UKM for allowing this research to be carried out and all supports that have been given throughout the process of this work. They would like to extend our appreciation towards KGC Sdn. Bhd. for sponsoring graphene flakes, Photonics

Technology Laboratory of Centre of Advanced Electronic and Communication Engineering (PAKET), Faculty of Engineering and Built Environment and Energy Conversion and Storage Materials Research Group of Solar Energy Research Institute for facilities provided.

REFERENCES

[1] M. A. Ismail *et al.*, "A fiber Bragg grating—Bimetal temperature sensor for solar panel inverters," *Sensors*, vol. 11, no. 9, pp. 8665–8673, 2011.
[2] V. Mishra, M. Lohar, and A. Amphawan, "Improvement in temperature sensitivity of FBG by coating of different materials," *Optik-Int. J. Light Electron Opt.*, vol. 127, no. 2, pp. 825–828, 2016.
[3] M. M. Elgaud, M. S. D. Zan, A. A. G. Abushagur, and A. A. A. Bakar, "Analysis of independent strain-temperature fiber Bragg grating sensing technique using OptiSystem and OptiGrating," in *Proc. IEEE 6th Int. Conf. Photon. (ICP)*, Kuching, Malaysia, Mar. 2016, pp. 1–3.
[4] A. J. Swanson *et al.*, "Investigation of polyimide coated fibre Bragg gratings for relative humidity sensing," *Meas. Sci. Technol.*, vol. 26, no. 12, p. 125101, 2015.
[5] C.-S. Park, K.-I. Joo, S.-W. Kang, and H.-R. Kim, "A PDMS-coated optical fiber Bragg grating sensor for enhancing temperature sensitivity," *J. Opt. Soc. Korea*, vol. 15, no. 4, pp. 329–334, 2011.
[6] A. D. Kersey, "A review of recent developments in fiber optic sensor technology," *Opt. Fiber Technol.*, vol. 2, no. 3, pp. 291–317, 1996.
[7] T.-C. Hsiao, T.-S. Hsieh, Y.-C. Chen, S.-C. Huang, and C.-C. Chiang, "Metal-coated fiber Bragg grating for dynamic temperature sensor," *Optik*, vol. 127, no. 22, pp. 10740–10745, 2016.
[8] Y. Li, Z. Hua, F. Yan, and P. Gang, "Metal coating of fiber Bragg grating and the temperature sensing character after metallization," *Opt. Fibre Technol.*, vol. 15, no. 4, pp. 391–397, 2009.
[9] W. Wu, Z. Qin, X. Liu, and T. Chen, "Investigation on low-temperature characteristics of FBG sensors and the technology to enhance sensitivity," in *Proc. Asia Commun. Photon. Conf. Exhib. (ACP)*, Shanghai, China, Dec. 2010, pp. 310–311.
[10] H. Khatoon and S. Ahmad, "A review on conducting polymer reinforced polyurethane composites," *J. Ind. Eng. Chem.*, vol. 53, pp. 1–22, Sep. 2017.
[11] M. S. Su'ait *et al.*, "The potential of polyurethane bio-based solid polymer electrolyte for photoelectrochemical cell application," *Int. J. Hydrogen Energy*, vol. 39, no. 6, pp. 3005–3017, 2014.
[12] L. Liu, X. Wu, and T. Li, "Novel polymer electrolytes based on cationic polyurethane with different alkyl chain length," *J. Power Sources*, vol. 249, pp. 397–404, Mar. 2014.
[13] S. Wang and K. Min, "Solid polymer electrolytes of blends of polyurethane and polyether modified polysiloxane and their ionic conductivity," *Polymer*, vol. 51, no. 12, pp. 2621–2628, 2010.
[14] M. Kumar, J. S. Chung, B.-S. Kong, E. J. Kim, and S. H. Hur, "Synthesis of graphene–polyurethane nanocomposite using highly functionalized graphene oxide as pseudo-crosslinker," *Mater. Lett.*, vol. 106, pp. 319–321, Sep. 2013.
[15] D. Cai, K. Yusoh, and M. Song, "The mechanical properties and morphology of a graphite oxide nanoplatelet/polyurethane composite," *Nanotechnology*, vol. 20, no. 8, p. 085712, 2009.
[16] P. Pokharel *et al.*, "Effects of functional groups on the graphene sheet for improving the thermomechanical properties of polyurethane nanocomposites," *Compos. B, Eng.*, vol. 78, pp. 192–201, Sep. 2015.
[17] C. S. Wong and K. H. Badri, "Chemical analyses of palm kernel oil-based polyurethane prepolymer," *Mater. Sci. Appl.*, vol. 3, no. 2, pp. 78–86, 2012.
[18] K. B. H. Badri, W. C. Sien, M. S. B. R. Shahrom, L. C. Hao, N. Y. Baderuliksan, and N. R. A. Norzali, "FTIR spectroscopy analysis of the prepolymerization of palm-based polyurethane," *Solid State Sci. Technol.*, vol. 18, no. 2, pp. 1–8, 2010.
[19] P. S. Kalsi, *Spectroscopy of Organic Compounds*. New Delhi, India: New Age Int. Pub, 2007.
[20] M. A. Corcuera *et al.*, "Effect of diisocyanate structure on the properties and microstructure of polyurethanes based on polyols derived from renewable resources," *J. Appl. Polym. Sci.*, vol. 122, no. 6, pp. 3677–3685, 2011.
[21] S. Chuayjuljit, T. Sangpakdee, and O. Saravari, "Processing and properties of palm oil-based rigid polyurethane foam," *J. Met., Mater. Minerals*, vol. 17, no. 1, pp. 17–23, 2007.
[22] X. Pan and D. C. Webster, "New biobased high functionality polyols and their use in polyurethane coatings," *ChemSusChem*, vol. 5, no. 2, pp. 419–429, 2012.
[23] M. Wang, C. Yan, and L. Ma, "Graphene nanocomposites," in *Composites and Their Properties*. London, U.K.: InTech, 2012, ch. 2, pp. 17–36.
[24] J. Liu and D. Ma, "Study on synthesis and thermal properties of polyurethane–imide copolymers with multiple hard segments," *J. Appl. Polym. Sci.*, vol. 84, no. 12, pp. 2206–2215, 2002.
[25] N. P. Apukhtina, *Methods for Increasing the Thermal Stability of Polyurethanes*. Technomic, Lancaster, PA, USA, 1973.
[26] X. Li, T. Hua, and B. Xu, "Electromechanical properties of a yarn strain sensor with graphene-sheath/polyurethane-core," *Carbon*, vol. 118, pp. 686–698, Jul. 2017.
[27] J. Phiri, P. Gane, and T. C. Maloney, "General overview of graphene: Production, properties and application in polymer composites," *Mater. Sci. Eng., B*, vol. 215, pp. 9–28, Jan. 2017.
[28] R. Baskaran, S. Selvasekarapandian, N. Kuwata, J. Kawamura, and T. Hattori, "Conductivity and thermal studies of blend polymer electrolytes based on PVAc–PMMA," *Solid State Ionics*, vol. 177, nos. 26–32, pp. 2679–2682, 2006.
[29] S. Ramesh and O. P. Ling, "Effect of ethylene carbonate on the ionic conduction in poly(vinylidenefluoride-hexafluoropropylene) based solid polymer electrolytes," *Polym. Chem.*, vol. 1, no. 5, pp. 702–707, 2010.
[30] S. K. Deraman, N. S. Mohamed, and R. H. Y. Subban, "Conductivity and dielectric properties of proton conducting poly (Vinyl) chloride (PVC) based gel polymer electrolytes," *Sains Malaysiana*, vol. 42, no. 4, pp. 475–479, 2013.

FAREEZA JASMI received the B.Sc. degree (Hons.) in electrical and electronic engineering from Universiti Kebangsaan Malaysia, Bangi, Selangor, Malaysia, in 2017. She is currently an Executive in industrial electronics at Denso (Malaysia) Sdn. Bhd.

NUR HIDAYAH AZEMAN received the B.Sc. degree in resource chemistry from Universiti Malaysia Sarawak in 2009, and the Master of Environment and Ph.D. degrees in smart sensing materials from Universiti Putra Malaysia in 2012 and 2017, respectively. She is currently a Post-Doctoral Researcher with the Centre of Advanced Electronic and Communication Engineering, Faculty of Engineering and Built Environment, Universiti Kebangsaan Malaysia, and her project focusing on the development of optical fiber sensor for environmental monitoring. Her current research interests include optical materials, and optical sensors and its applications.

AHMAD ASHRIF A. BAKAR (M'02–SM'12) received the bachelor's degree in electrical and electronics engineering from Universiti Tenaga Nasional in 2002, the M.Sc. degree in communications and network system engineering from Universiti Putra Malaysia in 2004, and the Ph.D. degree in electrical engineering from The University of Queensland, Australia, in 2010. He is currently an Associate Professor with the Centre of Advanced Electronic and Communication Engineering, Faculty of Engineering and Built Environment, Universiti Kebangsaan Malaysia. He is actively involved in the Optical Society of America and Fiber Optic Association Inc., USA. He is devoting his research work on optical sensors in environmental and biomedical application, specialized in plasmonic waveguide sensor, polymeric electro-optic modulator waveguide, interferometer, evanescent field sensors, and devices based on nanoparticles and nanostructures. He has been a member of OSA since 2014.

MOHD SAIFUL DZULKEFLY ZAN (M'15) received the bachelor's degree in electronics, information, and communication engineering from Waseda University, Japan, in 2006, and the master's and Ph.D. degrees from the Shibaura Institute of Technology, Japan, in 2011 and 2014, respectively. During his Ph.D. study, he proposed the optical pulse coding technique to improve the sensing performance of Brillouin optical time-domain analysis (BOTDA) fiber-optic sensor. He is currently a Senior Lecturer with Universiti Kebangsaan Malaysia. His research interests include Brillouin scattering-based fiber-optic sensors, such as BOTDA, BOTDR, optical pulse coding technique for fiber sensors, and Brillouin scattering-based fiber laser. He is also conducting research on fiber Bragg grating sensor.

KHAIRIAH HAJI BADRI received the bachelor's degree in chemistry and the B.E. degree in chemical and petroleum refining engineering from the Colorado School of Mines, USA, in 1993, and the Ph.D. degree in material sciences with a specialization in polymer synthesis and technology. She is currently a Professor with the Faculty of Science and Technology, School of Chemical Sciences and Food Technology, Universiti Kebangsaan Malaysia. She is also the Head of the Polymer Research Center, pioneering in thermosetting polymers from natural resources, such as palm oil, coconut oil, soybean oil, and agricultural biomass and converts them to polyurethanes. She is also intensively running a pre-commercialization project on the utilization of palm kernel oil and converted to polyol.

MOHD SUKOR SU'AIT received the B.Sc., M.Sc., and Ph.D. degrees in chemistry from Universiti Kebangsaan Malaysia (UKM), Malaysia, in 2007, 2010, and 2014, respectively. He is currently a Research Fellow with the Solar Energy Research Institute and an Associate Researcher with the Polymer Research Center, UKM. He had published about 15 papers in international refereed journal with an h-index, 5. His research interest in electrochemistry covers the synthesis and characterization of electrochemical materials for energy storage and conversion devices (lithium batteries and solar cell). In 2009, he has been selected as a Young Scientist to represent The Association of Southeast Asian Nations (ASEAN), in the 59th Nobel Laureates Meeting, dedicated to chemistry at Lindau, Germany, and honored as an ASEAN Scientist for Tomorrow by ASEAN at Jakarta, Indonesia, in 2009. He was a recipient of the Erasmus Mundus Mobility Program, University of Trento, Italy, in 2011, the Attachment Program at the Georgia Institute of Technology, USA, in 2012, and Cadi Ayyad University, Morocco, in 2014.